

UNCLASSIFIED

AD 4 2 3 3 9 1

DEFENSE DOCUMENTATION CENTER

FOR

SCIENTIFIC AND TECHNICAL INFORMATION

CAMERON STATION, ALEXANDRIA, VIRGINIA



UNCLASSIFIED

NOTICE: When government or other drawings, specifications or other data are used for any purpose other than in connection with a definitely related government procurement operation, the U. S. Government thereby incurs no responsibility, nor any obligation whatsoever; and the fact that the Government may have formulated, furnished, or in any way supplied the said drawings, specifications, or other data is not to be regarded by implication or otherwise as in any manner licensing the holder or any other person or corporation, or conveying any rights or permission to manufacture, use or sell any patented invention that may in any way be related thereto.

CATALOGED BY DDC
AS AD No. 423391

FZM-2951
4 November 1963

STRESS CORROSION CRACKING
OF
HIGH STRENGTH NICKEL ALLOY STEELS
FOR
AIRCRAFT APPLICATION

NOV 22 1963
RECEIVED
A A

Published and distributed under Contract No.
AF33(657)-11214, Air Force Materials Laboratory,
Aeronautical Systems Division, Air Force Systems
Command, Wright-Patterson Air Force Base, Ohio.

GENERAL DYNAMICS

GENERAL DYNAMICS | FORT WORTH

FZM-2951
24 June 1963

STRESS CORROSION CRACKING
OF
HIGH STRENGTH NICKEL ALLOY STEELS
FOR
AIRCRAFT APPLICATIONS

by
John F. Hildebrand

GENERAL DYNAMICS/FORT WORTH
A Division of General Dynamics Corporation
Fort Worth, Texas

TABLE OF CONTENTS

	<u>PAGE</u>
1. Figure and Table List	1
2. Abstract	1
3. Introduction	2
4. Materials	3
5. Test Specimen	5
6. Heat Treatment	8
7. Dry Film Lubricants	10
8. Corrosion Test	12
9. Stress Levels	13
10. Results	14
11. High Nickel Alloy Steels	19
12. Fractography	23
13. AISI 4340 and H11 Steels	25
14. Summary	35
15. Acknowledgments and References	38

FIGURE AND TABLE LIST

FIGURE	TITLE
1	One of the forgings used for this evaluation.
2	Stress corrosion specimen design
3	Typical stress corrosion fractures observed in specimens. A-18%Ni steel forging, B-9%Ni steel forging, C-H11 tool steel billet, D-AISI 4340 steel rod stock
4	The rock-candy like facets of the 18% Ni steel stress corrosion fractures
5	In the 18% Ni steel the intergranular attack was also seen as fissures in- to the fracture surface
6	Alternate immersion in dis-tilled water resulted in cracks at every boundary of 18% Ni steel.
7	Corrosion on H11 tool steel started as a pit which elongated to become a stress corrosion crack.
8	The intergranular attack was shown by the dark fissures in H11 tool steel fracture
9	Stress corrosion cracking shown as an intergranular attack in AISI 4340

FIGURE AND TABLE LIST (CONT'D)

FIGURE

TITLE

10

Surface of a stress corrosion crack in AISI 4340 rod stock. The origin was off to the upper left. Mode of fracture changed from intergranular to transgranular near the center above.

11

Stringers of inclusions, right center, were traced to the pit, left center, which was the origin of this stress corrosion crack in 9% Ni steel.

12

A band of corrosion in 9% Ni alloy was marked by pits resembling bored holes.

TABLE

TITLE

1

Chemical Composition of Materials

2

Heat Treatment of Test Materials

3

Tensile Strengths

4

Dry Film Lubricant Effect on AISI 4340 Rod Stock Tempered in the 263-290 ksi Range. Test Stress 200 ksi.

5

Tempered Strength Effect on the SCC Life of AISI 4340 Forgings

6

Tempered Strength Effect on the SCC Life of an H11 Tool Steel Billet.

FIGURE AND TABLE LIST (CONT'D)

TABLE	TITLE
7	Heat Treatment Effect on SCC Life of High Nickel Alloy Steels
8	Environment Effect on the SCC Life of High Nickel Alloys at the 260-290 ksi UTS.

STRESS CORROSION CRACKING
OF
HIGH STRENGTH NICKEL ALLOY STEELS
FOR
AIRCRAFT APPLICATIONS

Abstract

Forged parts and billets of AISI 4340, H11 tool steel, and 9% and 18% nickel alloy steels were evaluated for susceptibility to stress corrosion cracking (SCC) by an alternate immersion test. The alloys were prepared by the consumable electrode-vacuum melt practice and were heat treated as test specimens to strengths in the range from 263,000 to 290,000 psi. Polished specimens were alternately immersed in a 5% NaCl solution while sustaining a load equivalent to 75% of the ultimate strength.

A molydisulfide dry film lubricant curtailed the resistance to the SCC of AISI 4340; however, a chromic acid post treatment was restorative. This alloy disclosed a threshold to increasing susceptibility as the ultimate strength exceeded 200,000 psi. An H11 tool steel billet exhibited good resistance to SCC in the transverse direction. The 9% nickel alloy steel was more resistant to SCC than the 18% nickel alloy in either salt or distilled water. Both alloys were less susceptible than the AISI 4340 and were at least equivalent to the H11 tool steel.

Introduction

The aerospace industry needs information on the stress corrosion cracking (SCC) characteristics of high strength structural metals. Almost daily the mechanical properties of new alloys are presented to the designer for consideration as the material to use in some part of a space vehicle. Often, time does not permit the producers to make a comprehensive evaluation of the properties, particularly the corrosion and SCC characteristics. These new alloys cannot be subjected, practically, to all the environments which may be encountered by a vehicle during its service life. Since an aircraft experiences frequent and rapid changes of temperature, pressure, moisture, and stress, to name a few, the selection of a combination for an accelerated test of the SCC characteristics is difficult. Then the results of this accelerated test are necessarily limited to alerting the design engineer to the potential vulnerability of an alloy to SCC. The final proof of the structure is, unfortunately, determined by the service life.

The purpose of this paper is to report the results of a comparative analysis conducted by the Materials Laboratory of General Dynamics/Fort Worth on the SCC character-

istics of high strength nickel alloy steels, one of which is the maraging 18% nickel -9% cobalt alloy. The other important new structural materials are the 9% nickel -4% cobalt alloy and the type H11 tool steel. To complete the work previously reported by the author, Reference 1, some additional data are recorded for the SCC tendency of an AISI 4340 steel coated with a dry film lubricant.

Materials

Most of the test specimens for this program were cut from aircraft landing gear forgings such as the one shown by Figure 1. Basically, the shaped forgings were cylindrical, between 5 and 7 inches in diameter and from 20 to 36 inches in length. The final shapes were formed in a closed die forging press. All of the alloys were either mill annealed or, in the case of the 18% Ni forgings, one was solution heat treated and the other was "as forged". Aside from a sand blast clean up, the rough forgings had no other treatment prior to sectioning for the various evaluation test coupons.

The H11 type tool steel, however, was in the form of a forged billet, 4 x 12 x 20 inches, and some of the

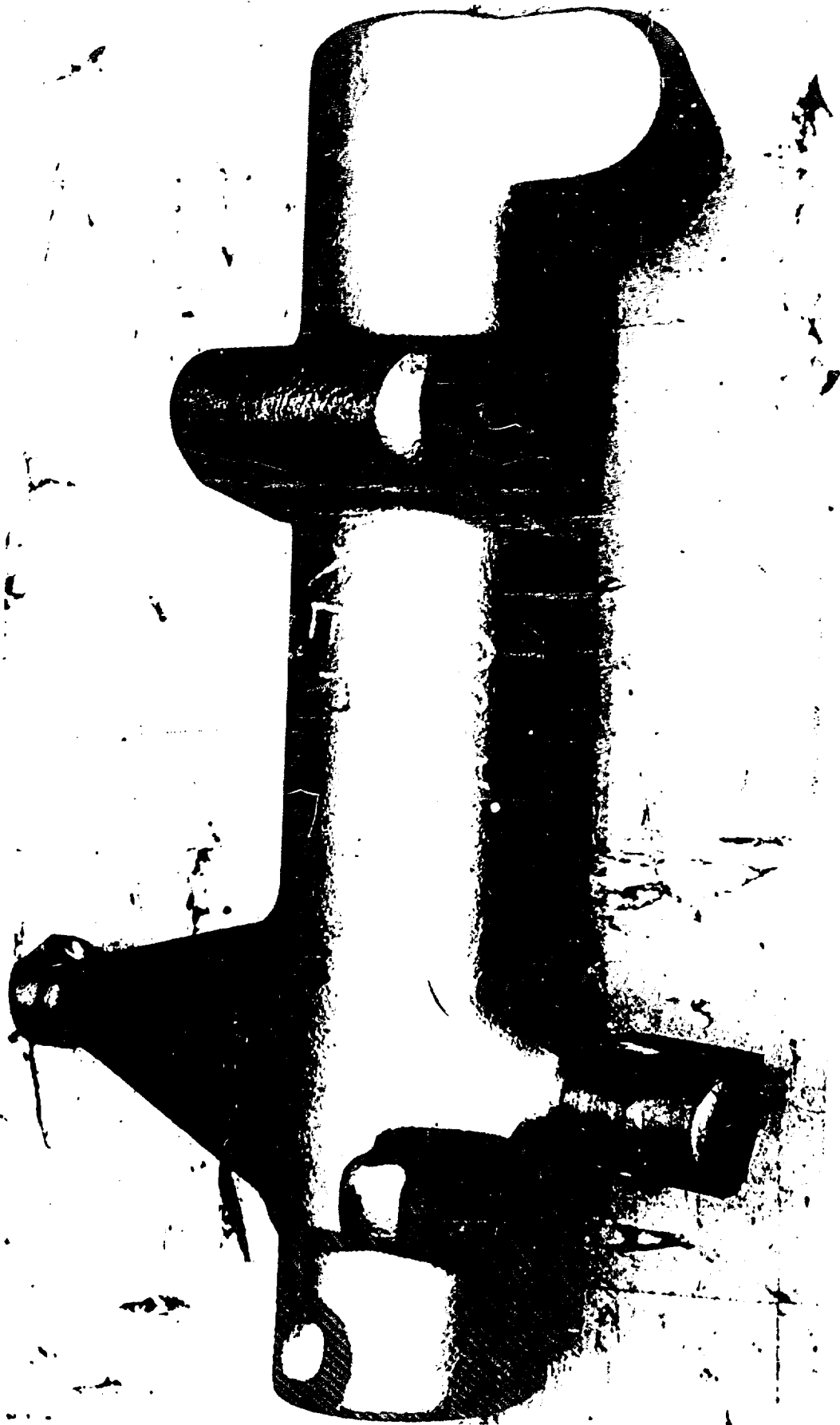


Figure 1 ONE OF THE FORGINGS USED FOR THIS EVALUATION

AISI 4340 rod stock which was from an air melt, all of the alloys had been prepared by the consumable electrode, vacuum melt process. These heats were made by different steel producers under the auspices of the U.S. Air Force. The chemical analyses, as shown by Table 1, conformed to the accepted specifications for the various alloys.

Test Specimen

Sufficient material was available from the several alloys to evaluate their susceptibility to SCC in both the longitudinal and short transverse grain directions. For the data presented here, the short transverse direction was perpendicular to the flash plane or die opening, while the longitudinal direction was parallel to it and the long dimension of the forging.

Figure 2 shows the specimen configuration which is a modification of the original design reported previously. This specimen has eliminated the problem of thread and shoulder-fillet failures. Where the corrosive media was previously excluded from the threads by a neoprene maskant, the seal was formed, in this test, between the shoulder and polyethylene container. The long shoulders also provided material for the machinist to back-off the cutting tool without the extra-revolution cut at the

TABLE 1
CHEMICAL COMPOSITION OF MATERIALS

ITEM		WEIGHT PERCENTAGE OF ELEMENTS											
	C	M _n	P	S	Si	Ni	Co	Mo	Cr	V	B	Al	Ti
18% NI- 9% Co Alloy	Forging O	.031	.004	.002	.06	19.11	9.00	5.18	-	-	.002	.04	.61
	Forging P	.025	.005	.003	.06	19.00	8.57	5.30	-	-	.002	.03	.61
	Forging S	.017	.006	.002	.07	19.24	8.36	4.84	-	-	.002	.07	.63
	Forging W	.016	.004	.002	.08	19.24	8.64	5.06	-	-	.002	.12	.63
	Nominal *	.03	.10	.01	.01	.10	18.50	9.00	4.90	-	-	.003	.10
9% Ni -4% Co Alloy	Forging M	.33	.001	.005	.02	8.70	3.76	.30	.31	.10			
	Forging N	.33	.002	.006	.02	8.82	3.83	.31	.31	.13			
	Forging T	.40	.002	.005	.03	8.94	3.86	.33	.33	.09			
	Forging V	.33	.002	.006	.02	8.82	3.79	.30	.31	.10			
	Nominal **	.04	.18	.01	.01	.10	8.5	3.75	.22	.22	.15		
AISI 4340 Alloy	Forging U	.41	.014	.006	.26	1.89	-	.23	.86	-			
	Rod Stock	.41	.003	.006	.26	2.02	-	.26	.86	-			
	Nominal ***	.40	.02	.013	.28	1.87	-	.25	.80	-			
Type H11 Tool Steel Alloy	Billet X	.36	.010	.006	.90	0.15	-	1.28	5.35	.66			
	Nominal ***	.40	.025	.025	1.00	-	-	1.30	5.00	.50			

* INCO ** Republic Steel *** AMS

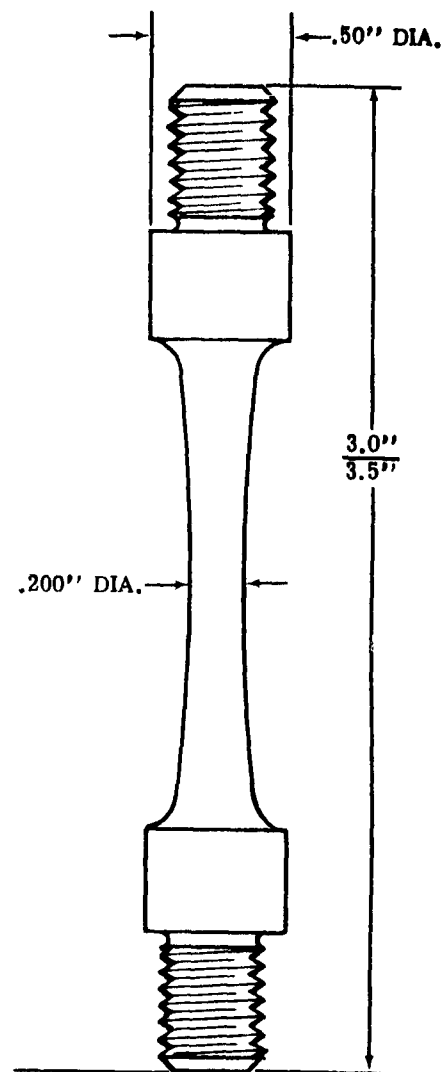


Figure 2 STRESS CORROSION SPECIMEN DESIGN

fillet tangency point. Tool marks resulting from this extra cut had formerly nucleated some of the stress corrosion cracks.

The specimens were finished to the final dimensions between the first and second draws. Following the second draw, there was a polishing operation which started with 320 grit emery cloth and ended with levigated alumina. Each specimen was macroscopically checked until the mirror-like surface was free of all gouges from the tool bit or emery paper.

A round specimen was selected for this investigation because it was easy to seal, isolated in the corrodant container, and it was easy to determine accurately the test loads. The stresses were, of course, tensile and axially applied by a modified stress rupture test machine.

Heat Treatment

Since this investigation was to evaluate four different alloys at several strength levels, the heat treatments necessarily involved a number of draw temperatures. These have been summarized in Table 2. The normalizing, austenitizing and solutioning treatments conformed to the material producers' recommendations, while the draw temperatures, particularly on the high nickel alloys, were selected on the basis of notch tensile strengths. This table

TABLE 2
HEAT TREATMENT OF TEST MATERIALS

MATERIAL	TREATMENT			
	NORMALIZE	AUSTENITIZE	QUENCH	TEMPER
AISI 4340	1650°F - 30 mins. (Neut. Atmos.)	1550°F - 30 mins. (Neut. Atmos.)	Oil @ 75-140°F	1. @ 400°F - 2 hrs. 2. Retemper @ 400, 475, 700, 800, or 900°F.
Type H11 Tool Steel		1850°F - 30 mins. (Insert Atmos.)	Air Cool	1. Double @ 1025°F - 2 hrs. each. 2. Final @ 1050, 1065, 1080, 1100 or 1135°F - 2 hrs. each.
9% Ni Alloy	1600°F - 60 mins.	1450°F - 60 mins.	Oil @ 75-140°F	1. @ 400°F - 1 hr. 2. Quench @ 1120°F - 2 hrs. 3. @ 400, 450, 550, or 700°F - 2 hrs. 4. Austquench @ 500°F - 8 hrs.
18% Ni	Solution Heat Treat @ 1500°F - 4 hrs.		Air Cool	1. @ 900 or 950°F - 3 hrs.

also shows that some of the 9% nickel alloy specimens were austquenched at 5000°F.

The tensile strength achieved by the various heat treatments are shown by Table 3. Note that the H11 tool steel tempers were not the same as were used on the SCC specimens. The latter were drawn at temperatures selected from a notch tensile strength temper temperature curves. In all cases, however, the tensile strengths agreed closely with published data for these alloys.

Dry Film Lubricants

The molybdenum disulfide dry film lubricant was applied to the AISI 4340 rod stock specimens after the final draw at 475°F. Each specimen was polished to remove all evidence of tool gouges before blasting with aluminum oxide. Using 60 psi air pressure, the 120 mesh oxide produced a soft matte finish of uniform texture. The specimens were washed in methyl ethyl ketone and vapor degreased in trichloroethylene, after which all handling was done with clean cotton gloves.

At this point in the process, three specimens were coated with the dry film lubricant. The rest were divided into two groups for precoating treatments. Group 1, while still hot from the degreaser, was submerged in a bath of Parco

TABLE 3
TENSILE STRENGTHS

MATERIAL	GRAIN DIREC.	TEMPER (°F)	ULT. STR. (ksi)	YIELD STR. (ksi)	RA (%)
AISI 4340 STEEL					
Rod Stock	long.	475	298	-	-
Forging	long.	475	268	222	48
Forging	trans.	475	262	216	14
Forging	trans.	700	237	-	-
Forging	trans.	800	204	-	-
Forging	trans.	900	186	-	-
Billet	trans.	475	268	-	-
TYPE H11 TOOL STEEL					
Billet	trans.	1050	268	223	40
Billet	trans.	1070	250	214	39
Billet	trans.	1080	265	228	36
Billet	trans.	1110	238	204	40
Billet	trans.	1125	221	203	43
18% NICKEL STEEL					
Forging W	trans.	900	288	261	45
Forging S	long.	900	284	273	17
Forging W	long.	950	292	283	38
9% NICKEL STEEL					
Forging T	long.	400	288	195	14
Forging T	long.	450	267	220	12
Forging V	long.	400	287	225	36
Forging V	trans.	450	271	216	26
Forging V	long.	450	275	223	38

Lubrite No. 2 which was maintained at 60 points concentration (60 ml of 0.1N NaOH to neutralize 1.0 ml of Parco solution), and at $205 \pm 2^{\circ}\text{F}$. Group 2 had the same treatment but in a 12-point bath. At the cessation of hydrogen evolution the specimens were immediately rinsed in hot running water for at least 10 minutes.

The dry film lubricant was applied to the room temperature specimens with an air operated spray gun until the film was from 0.0003 to 0.0005 of an inch thick. The two-stage cure cycle for this GD/FW-developed lubricant consisted of heating the specimens first at 260°F for 2 hours and then at 350°F for 12 hours. Sustained load, notched tensile data, as yet unpublished by GD/FW, have shown that the second stage bake was sufficient to preclude hydrogen embrittlement test failures.

Those specimens slated for the "post treatment" were dipped for 45 seconds in a hot (120°F) solution of chromic acid and then dried in a circulating air oven at 160°F for 30 minutes. The specimens were not rinsed following the chromic acid dip.

Corrosion Test

Details of the equipment and procedures for the corrosion test were reported in an NACE paper last year*. In this test

* Published as GD/FW Report FZM-2690. See Supplemental Sheets S-1, S-2 and S-3 for details of test procedures.

axially loaded specimens were sealed in polyethylene containers which were filled with a 5% solution of NaCl every 20 minutes. After being submerged for 5 minutes, the container was automatically drained, leaving the specimen exposed to the ambient container atmosphere for 15 minutes. This cycle was repeated until the specimen failed, or for a minimum of 200 hours. The solution was changed approximately every 48 hours at which time each container, reservoir, and connecting tube was rinsed without disturbing the film on the specimen.

Stress Levels

Most of the materials evaluated by this program were heat treated to an ultimate strength range of 263,000 to 290,000 psi. The sustained load on the corrosion specimens was fixed at 200,000 psi or between 68% and 77% of the ultimate strength. Where specimens with lower strength heat treatments were tested, the sustained load was calculated from 75% of the ultimate strength.

The type H11 tool steel was a special case. A potential service application for this material was designed to periodically sustain a stress near 200,000 psi. Therefore, all five of strength levels shown in Table 3 for this alloy were tested at that stress in order to ascertain their relative SCC susceptibility.

Results

Considering the effect of the dry film lubricant (DFL) treatments on the AISI 4340 rod stock specimens, it was noted as previously reported that the DFL and the pretreatments curtailed the life of the specimens, Table 4. The DFL coating without pretreatment reduced the life of the material on the average of 42%. Pretreatments both with and without the DFL had a much more drastic effect, shortening the specimen life by some 80 to 90%. In general, the 60-pt. solution caused a slightly greater loss in life than did the 12-pt. solution, but this was to be expected from the more vigorous chemical reaction of the more concentrated solution. Both solutions pitted the specimen surface. The notches created by these pits varied in size and location such that it was difficult to determine their direct effect on an individual specimen. Nevertheless, it seemed reasonable to assume that the stress concentration produced at these pits was at least in part responsible for the differences noted in the life of the specimens.

The post-treatment of a chromic acid bath was ineffective in protecting a specimen treated in the 60-pt. solution but actually restored and prolonged the life of the 12-pt. pretreated specimens, three of which exceeded twice the life of the control specimens, Table 4.

TABLE 4

Dry Film Lubricant Effect on AISI 4340 Rod
 Stock Tempered in the 263-290 ksi Range.
 Test Stress 200 ksi.

SURFACE TREATMENT	TIME-TO-FAILURE (hours)
Control - Bare Specimen DFL - No Pre or Post- Treatment	197.3, 244.6, 290.1 155.1, 146.1, 119.8
Pretreatment (60-pt. Sol.), No DFL Pretreatment (12-pt. Sol.), No DFL	2.6, 19.1, 14.5 51.8, 29.8, 0.3 (?)
Pretreatment (60-pt. Sol.) + DFL Pretreatment (12-pt. Sol.) + DFL	10.5, 14.0, <30** .9***, 153.1, 7.5
Pretreatment (60-pt. Sol) + Post-Treatment + DFL Pretreatment (12-pt. Sol) + Post-Treatment + DFL	.2, 2.1, 7.4 NF*, NF*, NF*

* No failure, life exceeded 500 hours

** Malfunction of timer

*** Thread failure from quench crack

By comparison the longitudinal specimens from the AISI 4340 forging, Table 5, had a much greater susceptibility to SCC than the rod stock control specimens, Table 4. Even shorter were the lives of the transverse specimens. In fact, the three different forgings all had very short lives in the high strength condition.

It would seem that AISI 4340 billet and forged materials have a definite threshold temperature near 800°F above which the susceptibility to SCC was definitely curtailed. Of the specimens drawn at 700°F only the billet material showed a slight improvement in the resistance to SCC. Drawing at 800°F, however, produced a marked increase in specimen life, and after a 900°F draw, only one of the specimens had failed after 200 hours exposure to the alternate immersion test.

As mentioned previously, the type H11 tool steel was considered a special case. Only billet material was available for the test and only one stress, 200,000 psi, was applied to the specimens heat treated to the several strength levels evaluated. Table 6 shows that at the highest strength type H11 specimens were slightly better than the AISI 4340 billet. As the ultimate strength was reduced by higher tempering temperatures, the susceptibility

TABLE 5
TEMPERED STRENGTH EFFECT ON THE SCC LIFE OF AISI 4340 FORGINGS

ITEM	GRAIN DIRECTION	TEMPER (°F)	UTS (ksi)	STRESS (ksi)	TIME-TO-FAILURE (hours)
Forging (1)	long.	475	-	200	83.8, 22.3*, 49.9, 28.6
Forging (1)	trans.	475	273	200	0.4, 0.3, 0.1
Forging (2)	trans.	475	-	200	0.1, 0.1, 0.4
Forging (3)	trans.	475	-	200	0.2, 0.3, 0.2
Billet	trans.	475	268	200	1.7, 0.6, 4.1
Billet	trans.	700	237	173	10.5, 10.4
Forging (1)	trans.	700	-	173	0.6, 6.3, 0.5, 0.3
Forging (2)	trans.	700	-	173	0.4
Forging (3)	trans.	700	-	173	0.4
Billet	trans.	800	206	158	23.8, NF**
Forging (1)	trans.	800	-	158	2.2, 63.8, 39.3, 150.1
Forging (2)	trans.	800	-	158	25.4, NF
Forging (3)	trans.	800	-	158	47.5
Billet	trans.	900	192	144	NF, NF
Forging (1)	trans.	900	-	144	NF, NF, NF
Forging (2)	trans.	900	-	144	NF, NF
Forging (3)	trans.	900	-	144	NF

* thread failure ** no failure after 200 hours

TABLE 6
TEMPERED STRENGTH EFFECT ON THE SCC LIFE
OF AN H11 TOOL STEEL BILLET

ITEM	TEMPER (°F)	TEST STRESS (ksi)	TIME-TO-FAILURE (hours)
Billet	1050	200	13.0, 16.2, 19.3
Billet	1065	200	16.2, 20.5, 10.0
Billet	1080	200	40.3, 33.5, 29.6
Billet	1100	200	82.5, 88.5, 103.0
Billet	1135	200	70.1, 141.5, 249.0

to SCC decreased. Had the test stress been reduced so as to maintain it at 75% of the ultimate strength, the material drawn at the higher temperatures, in all probability, would have exhibited an even greater decrease in susceptibility to SCC.

High Nickel Alloy Steels

Consider now the SCC of the 9% and 18% nickel alloy steels. Of the first four forgings received, the notched to unnotched ultimate strength ratios, as yet unpublished by GD/FW, indicated that the 9% Ni "T" and 18% Ni "S" forgings had apparently been overheated during forging.

Table 7 shows that the "T" forging was far more susceptible to SCC than the companion "V" forging which had not been overheated. On the other hand, overheating had produced a negligible difference in the 18% Ni companion forgings "S" and "W". These same forgings as listed in Table 7 were also compared after tempering specimens at two temperatures and although some slight difference was observed in the tensile properties, the SCC susceptibility for a given forging was essentially the same.

The overheated forgings were replaced by one 9% Ni -"N" forging and one 18% Ni -"P" forging, which when tested

TABLE 7

HEAT TREATMENT EFFECT ON SCC
LIFE OF HIGH NICKEL ALLOY STEELS

ITEM	DRAW TEMP. (°F)	TEST STRESS (ksi)	TIME-TO-FAILURE (hours)	AVERAGE
<u>9% Nickel</u>				
Forging V	400	200	23.1, 48.2, 129.6	67
Forging V	450	200	26.5, 46.4, 128.1	67
Forging T**	400	200	24.5, 17.2, 2.7	19
Forging T**	450	200	30.8, 5.8, 19.4	15
Forging N	450	200	11.7, 46.3, 91.7, 65.2, 53.8, 162.9	67
Forging N	550	186	86.1, 139.4, 146.5	124
Forging N	700	169	NF*, NF	
Forging N	500 EQ	186	NF, NF	
<u>18% Nickel</u>				
Forging W	900	200	5.5, 10.1, 7.6	8
Forging W	950	200	9.0, 10.0, 5.1	8
Forging S**	900	200	16.9, 5, 4.1	9
Forging S**	950	200	7.6, 10.1, 5.5	14
Forging P	900	200	8.5, 7.3, 5.7, 24.8, 25.3	14

* No failure after 200 hours ** Material overheated
during forging.

produced results substantiating the test data, from the "V" and "W" forgings, respectively. On the average, the 9% Ni alloy had about one-fifth of the susceptibility to SCC that the 18% Ni alloy had. Compared with AISI 4340 rod stock as the base, both of the high nickel alloys were decidedly better, but the 9% Ni alloy was superior.

Also included in this investigation of the susceptibility of high nickel alloys to SCC was the effect of heat treatment, corrosion media, and grain structure. Table 7 shows the data obtained from the 9% Ni -"N" forging specimens which were drawn at 550°F and 700°F and austquenched at 500°F. Those drawn at 550°F exhibited an average longevity 80% better than those drawn at 450°F. Drawing at 700°F and austquenching at 500°F produced further improvements; none of these specimens failed after 200 hours exposure.

Some specimens of the 18% Ni and 9% Ni alloy forgings and the 18% Ni rod stock were exposed to distilled water instead of salt water. Table 8 shows that, as expected, the stress corrosion cracking susceptibility was much greater in the salt water. The data again points out how the 9% Ni forging short transverse specimens have more resistance to SCC than the 18% Ni forging specimens in either the short transverse or longitudinal grain direction.

TABLE 8

ENVIRONMENT EFFECT ON THE SCC LIFE OF
HIGH NICKEL ALLOYS AT THE 260-290 ksi UTS

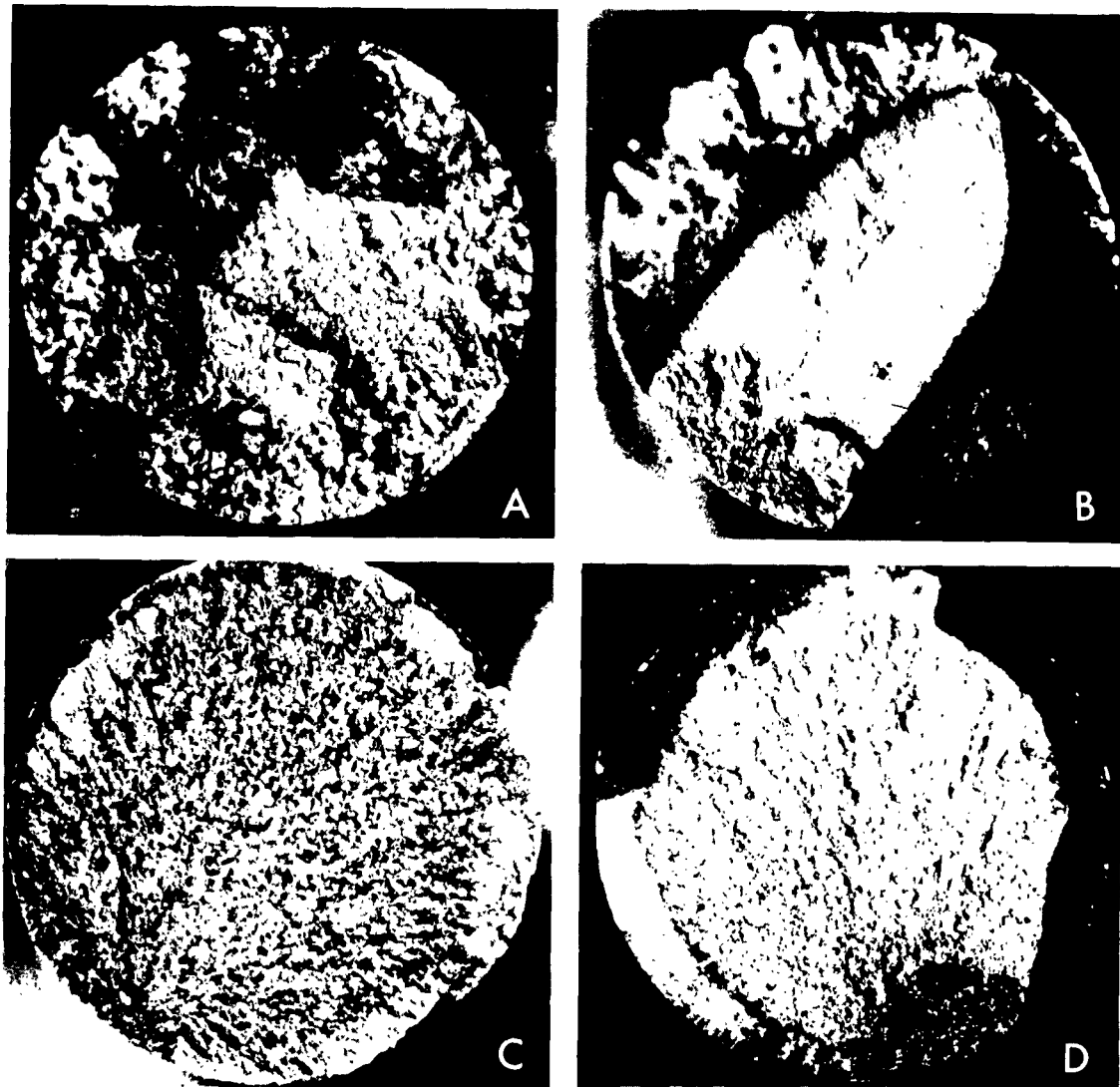
ITEM	GRAIN DIREC.	ENVIRONMENT (water)	TIME-TO-FAILURE (hours)
<u>18% Nickel</u>			
Forging P	s.t.	5% Salt	5.1, 6.2, 4.1, 5.4
Forging P	s.t.	Distilled	42.3, 8.3*
Forging O	s.t.	5% Salt	12.7, 12.2, 7.9, 11.1
		Distilled	185.3, 150.7*
Forging P	long.	5% Salt	15.0, 12.7
Forging O	long.	5% Salt	28.3, 49.7
Rod Stock	long.	5% Salt	76.8, 75.9
Rod Stock	long.	Distilled	316.8, NF**
<u>9% Nickel</u>			
Forging N	s.t.	5% Salt	46.7, 106.5, 48.1, 121.9
Forging N	s.t.	Distilled	NF, NF

* Thread failure ** No failure after 400 hours

Fractography

Occasionally there was time after a specimen broke to rinse and dry it before rust obliterated the fracture texture. A typical fracture from each of the alloys being tested during this program is shown in Figure 3. Compare these fractures with the evidence of ductility, fracture texture, and mode of attack.

The H11 tool steel exhibited a brittle fracture characterized by the large flat plane of catastrophic crack propagation and by the very small shear lip. Brittleness, however, was not seen in the 18% Ni fracture although it had no obvious shear lip. Extensive intergranular attack girdled the specimen and precluded the formation of any shear lip, but ductility was revealed by the rugged texture at the center of the fracture. Between these two fracture extremes were those of the AISI 4340 and the 9% Ni alloy. Both exhibited a considerable shear lip which resembled the cup-cone tensile fracture of a ductile metal, and a fracture texture which depicted the fine grain of these two alloys. Although only a single crescent of SCC attack was usually found in most of these uniplanar fractures, a few exhibited smaller, secondary crescents at various places on the shear lip.



MAG. 13X

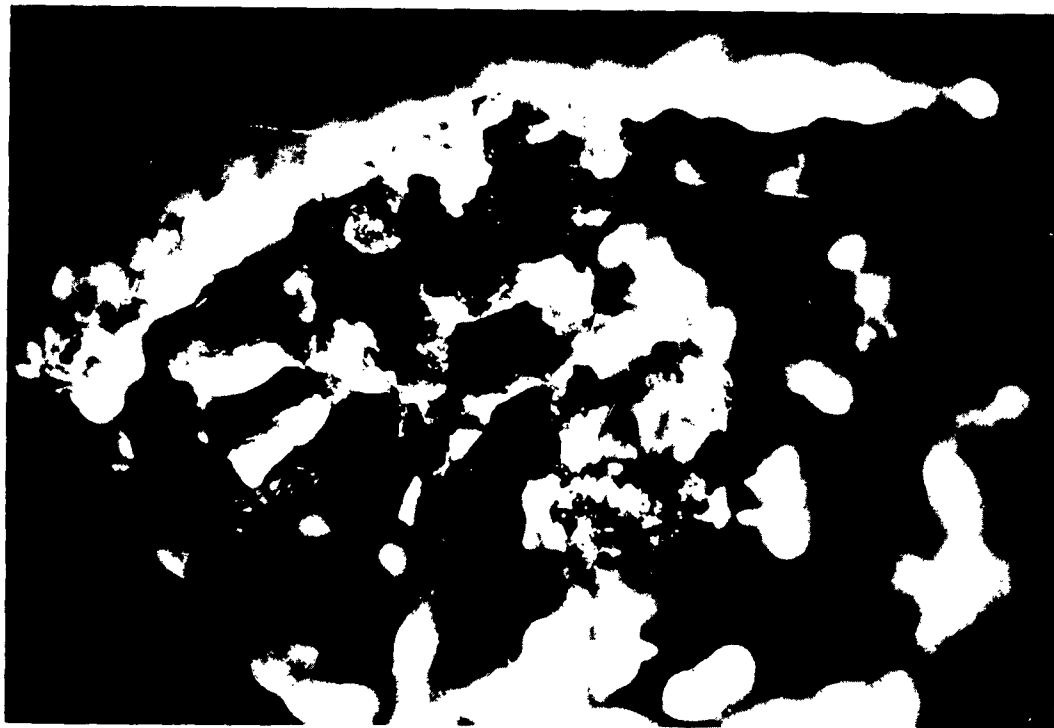
Figure 3 TYPICAL STRESS CORROSION FRACTURES OBSERVED IN SPECIMENS. A - 18% Ni STEEL FORGING, B - 9% Ni STEEL FORGING, C-H11 TOOL STEEL BILLET, D - AISI 4340 STEEL ROD STOCK.

The 18% Ni alloy fracture, on the other hand, exposed the many crescent origins indicative of circumferential stress corrosion cracking, or ubiquitous attack which resulted in a multilevel fracture. The shear lip evidence of ductility became the shear cliffs connecting the various levels of the fracture surface. To the unaided eye the SCC crescents revealed coarse grains.

Optical fractographs of the stress corrosion cracking in the 18% Ni alloy, Figures 4 and 5, showed the rock-candy like facets of the grains and intergranular fissures penetrating the fracture plane. On the polished surface of this test specimen, the SCC was barely visible as a mesh of fine hairlines. The full extent of the damage done even by alternate immersion in distilled water was revealed by a photomicrograph of the section through the specimen surface. The attack was definitely intergranular beginning at almost every grain boundary, Figure 6.

AISI 4340 and H11 Steels

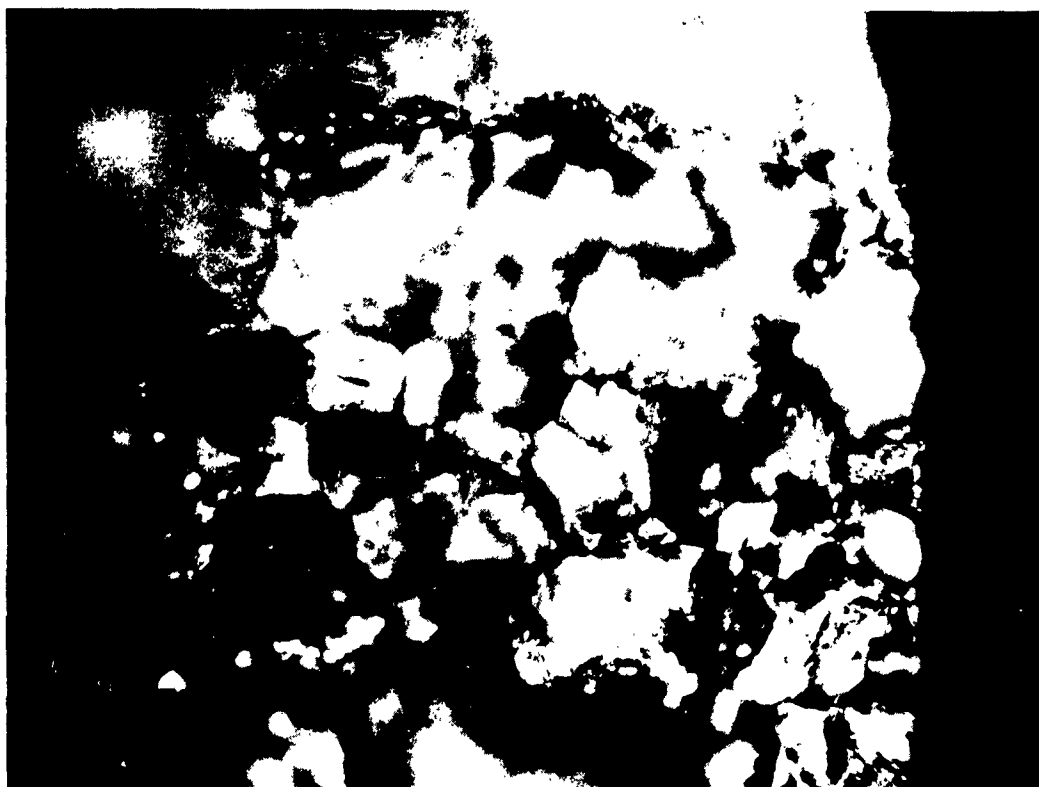
When exposed to the salt water, the surface of both the H11 tool steel and the AISI 4340 rod stock developed a uniform coating of rust with only occasional pits. The H11 specimens, being transverse from a billet, developed



MAG. 150X

DARK FIELD

Figure 4 THE ROCK-CANDY LIKE FACETS OF THE 18% Ni STEEL
STRESS CORROSION FRACTURES.



MAG. 200X

DARK FIELD

Figure 5 IN THE 18% Ni STEEL THE INTERGRANULAR ATTACK WAS ALSO SEEN AS FISSURES INTO THE FRACTURE SURFACE.



MAG. 100X

Figure 6 ALTERNATE IMMERSION IN DISTILLED WATER RESULTED IN
CRACKS AT EVERY GRAIN BOUNDARY OF 18% Ni STEEL.

pits at numerous exposed inclusions, Figure 7. As the pits formed, they quickly elongated to become a slot and then a crack transverse to the applied stress, but enlargement of the crack by intergranular attack was cut short by a catastrophic propagation. Optical fractography of the stress corrosion crescent disclosed the intergranular nature of the attack in the H11 tool steel, Figure 8.

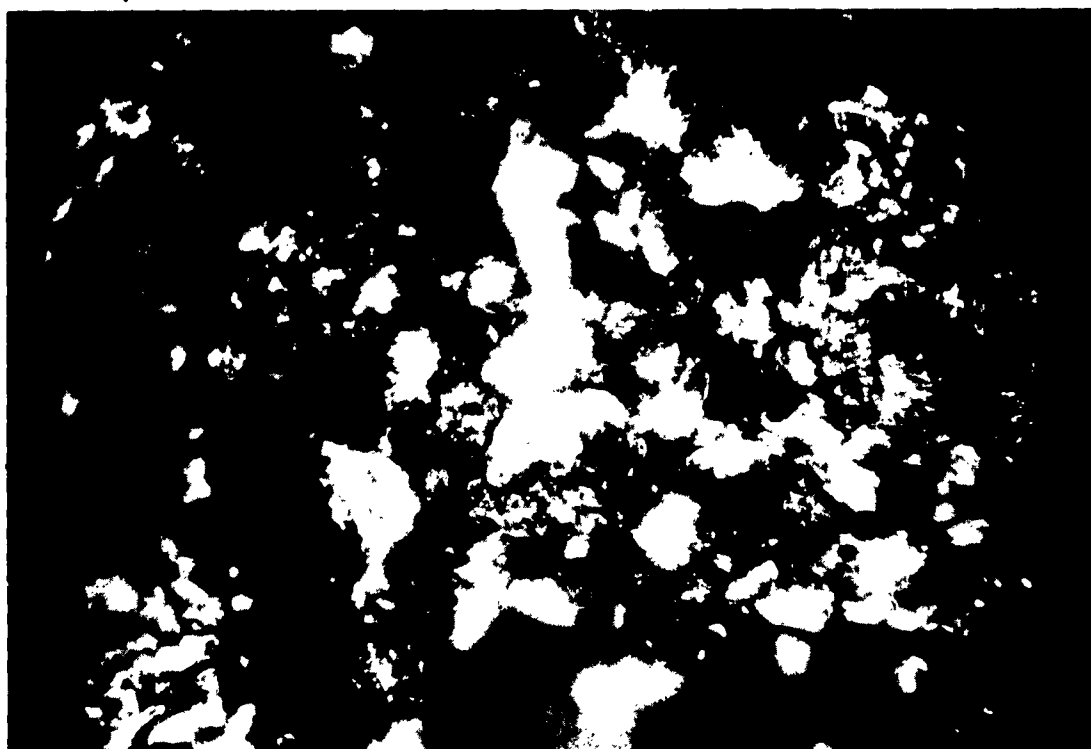
Although pits formed in the AISI 4340, it was difficult to find any direct evidence of a connection with origin of failure. Stress corrosion was seen as a crescent in the fracture, Figure 3 D, and as an intergranular attack in the microstructure, Figure 9. Optical fractography was only able to disclose the transition from the intergranular crescent texture to the cleavage fracture texture as shown in Figure 10.

One of the 9% Ni alloy fractures exhibited the distinctive feature of a string of inclusions which were traced to the origin of the SCC. At higher magnification, Figure 11, the trail of these inclusions lead directly to the pit from which the action began. A series of inclusion stringers must have existed at this point in the forging because similar pits formed a line of corrosion along



MAG. 13X

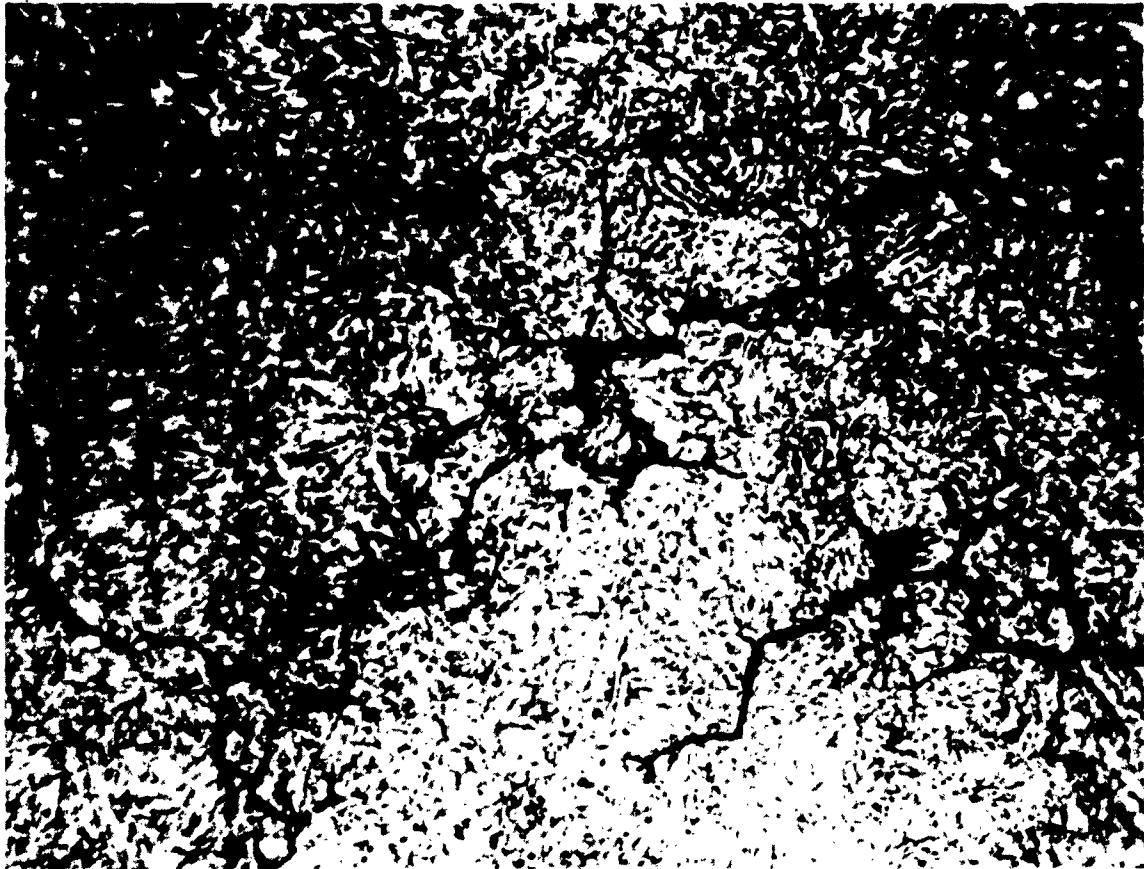
Figure 7 CORROSION ON H11 TOOL STEEL STARTED AS A PIT WHICH
ELONGATED TO BECOME A STRESS CORROSION CRACK.



MAG. 200X

DARK FIELD

Figure 8 THE INTERGRANULAR ATTACK WAS SHOWN BY THE DARK FISSURES IN THE H11 TOOL STEEL FRACTURE.



MAG. 2000X

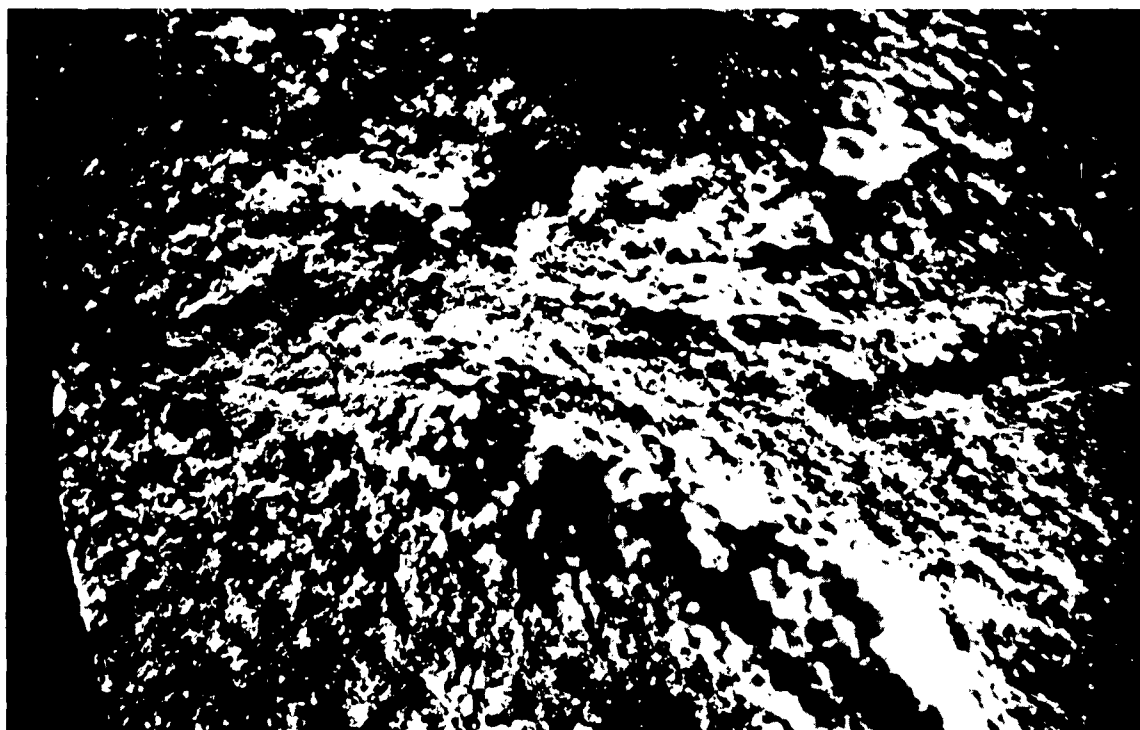
Figure 9 STRESS CORROSION CRACKING SHOWN AS AN INTERGRANULAR
ATTACK IN AISI 4340.



MAG. 100X DF

DARK FIELD

Figure 10 SURFACE OF A STRESS CORROSION CRACK IN AISI 4340 ROD STOCK. THE ORIGIN WAS OFF TO THE UPPER LEFT. MODE OF FRACTURE CHANGED FROM INTERGRANULAR TO TRANSGRANULAR NEAR THE CENTER, ABOVE.



MAG. 100X

DARK FIELD

Figure 11 STRINGERS OF INCLUSIONS, RIGHT CENTER, WERE TRACED TO THE PIT, LEFT CENTER, WHICH WAS THE ORIGIN OF THIS STRESS CORROSION CRACK IN Ni STEEL.

the length of the test specimen, Figure 12. Adjacent to the corrosion, the test surface was unmarred by oxidation, but where each string came to the surface, the rapid anodic attack resembled a bored hole. Such an attack was thought to be an unlikely cause of failure in a serviceable forging unless some machined surface or unusual grain flow pattern exposed the inclusions to a corrosive environment.

Summary

To conclude the work started with dry film lubricants on AISI 4340 and reported previously, it has now been shown that DFL both with or without a pretreatment increased the susceptibility to SCC in the high strength range. A post-treatment of chromic acid partially restored the resistance of this alloy to corrosive attack.

AISI 4340 revealed a threshold of susceptibility, those forging specimens drawn at 800°F and 900°F had a resistance to stress corrosion cracking at least 25 times greater than those drawn at 475°F and 700°F. The resistance to SCC was poor when the ultimate strength of this alloy exceeded 200,000 psi.

The H11 type tool steel exhibited a relatively good resistance to stress corrosion cracking, particularly, if



MAG. 13X

Figure 12 A BAND OF CORROSION ON 9% Ni ALLOY WAS MARKED BY PITS RESEMBLING BORED HOLES.

the tempering temperatures used for the triple draw finished above 1050°F, or an ultimate strength near 260,000 psi.

By comparison with the AISI 4340, both the 18% Ni and the 9% Ni alloys had better resistance to SCC in their optimum strength ranges. The 9% Ni alloy was better than the 18% Ni alloy in both salt water and distilled water.

These results record the relative resistance to stress corrosion cracking of the four alloys as evaluated by alternate immersion tests, but the data should only be used as guides by a design or materials engineer until actual tests can be conducted in the service environment.

Acknowledgements

The author wishes to thank General Dynamics/Fort Worth for permission to present this paper for publication and the people of the Materials Laboratory for their invaluable assistance.

This program was authorized under U.S. Air Force Contracts 33(600)-36200 and 33(600)-41891.

References

1. F. Nordquist, E. Turns, and J. Hildebrand.
Stress Corrosion Cracking in High Strength Ferrous Alloys. Presented at Southwest Regional Meeting of NACE in 1962.



DESCRIPTION OF TEST PROCEDURES

A battery of 23 sustained load test machines was available for the typical stress corrosion setup shown by Figure S-1. An axial load on the specimen was obtained by dead weights acting through a 20:1 lever arm. The arm was balanced over a knife edge fulcrum and the specimen was suspended between upper and lower extension rods. Alignment of the specimens was maintained by a gimbal between the lever arm and rod. Integral with the machine was an automatic timer which marked tenths of hours until failure occurred.

Hastelloy grips were pin connected to the extension rods and the lower grip was enclosed by the polyethylene container. Figure S-2 shows the details of the grip and container. A polyethylene cover minimized evaporation of the solution and restricted the splash when a specimen broke.

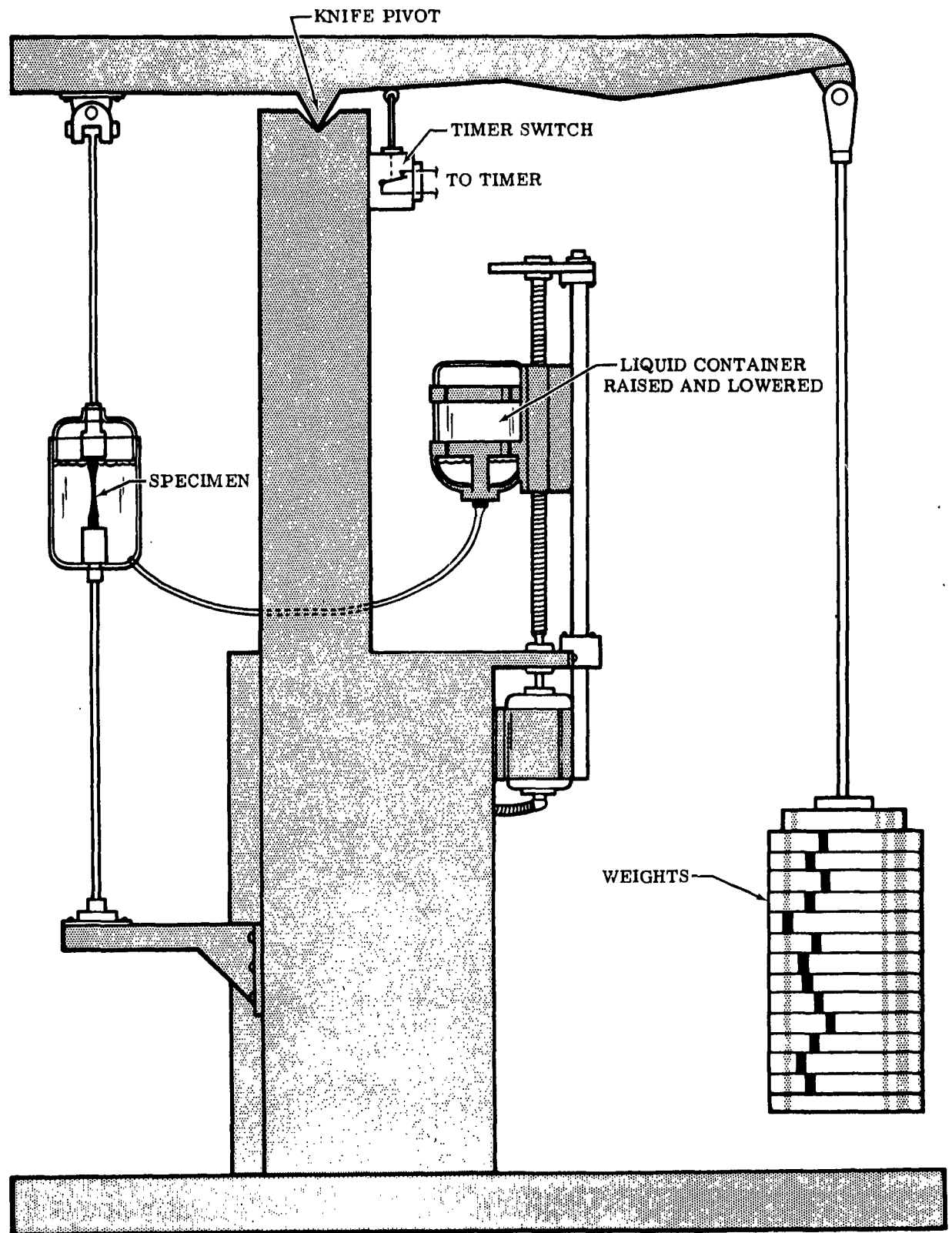


Figure S-1 STRESS CORROSION TEST FIXTURE SCHEMATIC

FW 62 171 P002

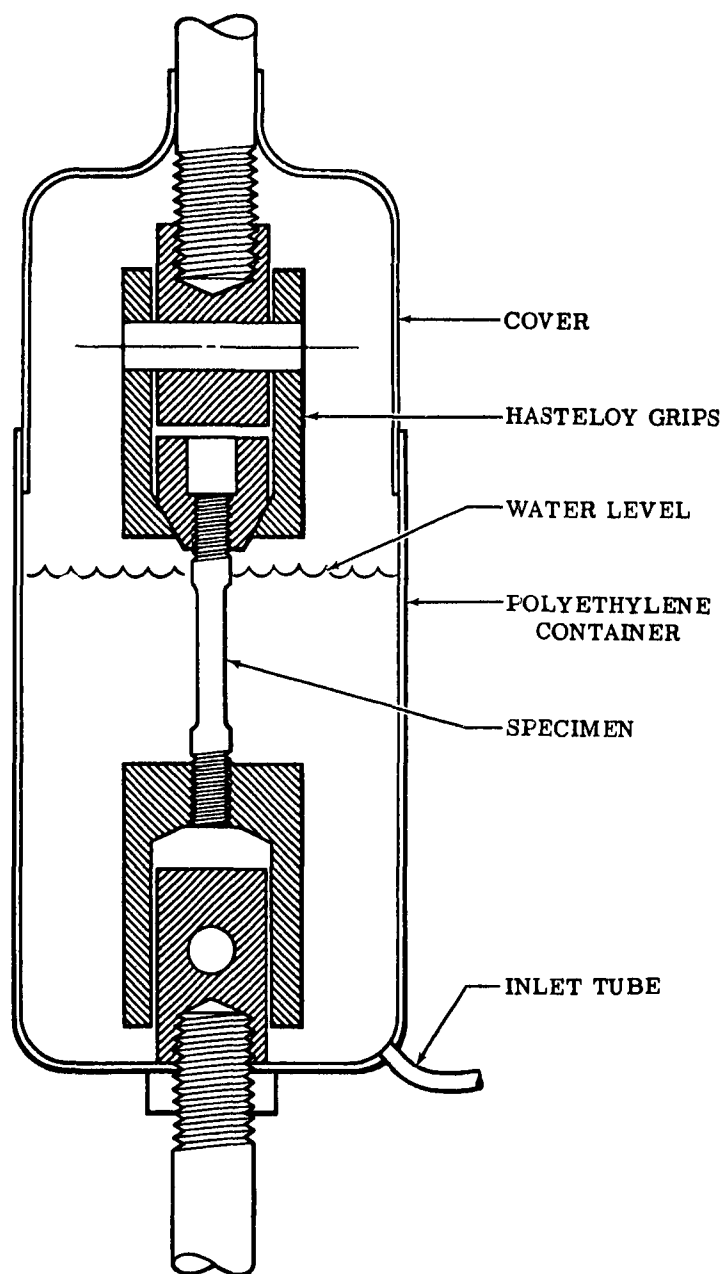


Figure S-2 GRIP FIXTURES AND CONTAINER FOR STRESS CORROSION TEST

FW 62 171 P003